

# Classicality of Spin Coherent States via Entanglement and Distinguishability

D. Markham and V. Vedral

Optics Section, Blackett Laboratory, Imperial College, London SW 7 2BW, United Kingdom.

(Dated: February 9, 2020)

We trace the properties of spin coherent states as we vary  $S$  through  $S = 1/2, 1, \dots$  in two respects: in their resistance to entanglement generation (when passed through a beam splitter) and in the distinguishability of the states. In the infinite  $S$  limit the spin coherent state is a subclass of the optical coherent states, namely, the subclass of orthogonal optical coherent states. These states generate no entanglement and are obviously completely distinguishable. This transition is discussed in terms of the classicality of the states. The decline of the generated entanglement, and in this sense increase in classicality with  $S$ , is very slow and dependent on the amplitude  $z$  of the state. Surprisingly we find that, for  $|z| > 1$ , there is an initial increase in entanglement followed by an extremely gradual decline to zero. The distinguishability, on the other hand, quickly becomes apparent and in this sense classical for all  $z$ . We illustrate the distinguishability of spin coherent states in a novel manner using the representation of Majorana.

## I. INTRODUCTION

The transition from the quantum to the classical world is not fully understood at present. Although classical physics is believed to be a limiting case of quantum mechanics, it is frequently unclear which limit should be taken and how this is to be achieved. We can, for example, try to think of how the laws of physics come to appear as the classical laws if we start from the Schrodinger equation, as in [1]. Alternatively, we might think about how physical objects themselves come to appear classical, when they are so manifestly quantum at the most basic level that we can test in our most accurate experiments. In this case, initial quantum states describing objects would somehow have to make a transition to become classical. Quantum physics has been considered to approach the classical in many different ways and we name several of them: 1) As  $\hbar$  goes to zero, the variance (or uncertainty) of a measurement goes to zero and we can separate all states perfectly (this is known as Bohr's correspondence principle); also, the classical Hamilton-Jacobi dynamics can be "derived" from the Schrodinger equation in this limit. 2) Positivity of the Wigner or P-function is often taken to imply classicality, since they then can be thought of as representing real probability functions as in classical statistical mechanics. 3) The entanglement present in a collection of states is clearly an indication of nonclassicality and a lack of it can be construed as a signature of classicality (various decoherence pictures, on the other hand, use the entanglement with the environment as an indication of classicality; in this case the global presence of entanglement leads to classicality). 4) Distinguishability of states (classical states are always fully distinguishable at least in principle). Although each of these criteria is adequate in its own domain, it needs to be stressed that they are by no means equivalent. In fact, they frequently contradict each other. A well known example of this is that a state of two light modes can be entangled and still have an overall positive Wigner function, as well as vice versa. It is, therefore, very important to investigate the relationship between these various approaches in order to gain a deeper understanding of the transition between the quantum and the classical. In this paper we trace the spin coherent state through a range of spin  $S$ , from  $S = 1/2$  to the limit  $S \rightarrow \infty$ , and comment on this as a transition to classicality for this class of pure states.

One of the first set of states defined specifically with classicality in mind is the optical coherent states or Glauber states [2]. These are minimum uncertainty states and, in addition to the fact that they can be created from classical electromagnetic fields, they can be seen to be classical in two of the respects mentioned above. The first way can be seen in their action through a beam splitter. It has been proven that the Glauber states are the only pure states that when passed through one arm of a beam splitter (with the other arm being a vacuum) return product states, which are states with zero entanglement [3]. In this way the classical feature of no entanglement is maintained when the state passes through a beam splitter. Secondly, and speaking somewhat loosely, as their amplitude tends to infinity (meaning that the number of photons becomes arbitrarily large), all Glauber states become orthogonal to one another and therefore distinguishable. In this way, we can think of a laser beam of many photons as completely distinguishable from another such laser beam.

The Glauber states can then be generalised in different ways to a wider set of states, including minimum-uncertainty-defined states and group-defined states (see [4] and [5] for good reviews). One such generalisation is the set of spin coherent states, introduced in [6] and [7], which have been compared to the Glauber states and some parallels drawn. For example, they too are states of minimum uncertainty and they can be produced by classical fields. As the size of the spin  $S$  limits to infinity, the spin coherent states limit to the set of orthogonal Glauber states. In this paper, we extend this comparison of the spin coherent states to looking at the transition as we change the size of the spin from  $S = 1/2$  to the limit  $S \rightarrow \infty$  Glauber states. This is done with respect to their robustness against entanglement

created through a beam splitter and their distinguishability, using the Helstrom measurement strategy. As well as being interesting in their own right, these properties allow us to investigate how quickly the classical features of the Glauber states mentioned above appear. We discuss the transition as an approach to this classicality, considering the "most classical" to be the limiting orthogonal Glauber states. We note however, that this is of course not the whole story for classicality. We deal here only with pure states, and classically, we can only truly model mixed states. Indeed even then the states are, of course, still quantum and they only behave like classical states if the quantum features are small enough to be ignored. In this paper we talk about classicality in a very specific sense, namely, in entanglement and distinguishability, for which, in the specific scenarios discussed, the Glauber state is the most classical-like among the set of pure spin coherent states. In this sense, we trace the spin coherent state from what we think of as the "least" classical,  $S = 1/2$ , to the "most" classical  $S \rightarrow \infty$ .

In particular, in section II we investigate the entanglement of the state generated by passing it through one arm of a 50/50 beam splitter while the other arm is left in the empty vacuum state. It is known that, in the infinite spin limit, spin coherent states are a subclass of the Glauber states ([6],[7]). Thus in the infinite limit the generated entanglement goes to zero. We present a different proof in terms of the states in the first quantisation. Our method has the advantage that it easily follows that there are infinitely many other states of the same dimensionality as spin coherent state with the same property that they asymptotically approach the Glauber states. We find that the reluctance to entanglement generation is very slow to increase with  $S$  and the entanglement is only near zero for very high  $S$ . In addition, the entanglement generation is dependent on  $z$  and for  $|z| > 1$  we see a surprising rise in entanglement - hence decline in classicality. This is explained and parallels drawn to another similar case noted by A mesen et al [8]. The validity of this as a measure of classicality is then discussed.

In section III, we investigate the change in distinguishability of the state with the spin  $S$  in terms of the probability of error for a Helstrom optimal measurement. We find that the probability of error decreases rapidly with  $S$ , hence the distinguishability increases rapidly to a maximum level. We discuss this as a measure of the transition to classicality for the spin coherent state. Thinking only of classicality in terms of how distinguishable two states are, this transition is smooth and quick from the least classical spin  $1/2$  state to the most classical limit  $S \rightarrow \infty$ . We then go on to look at the Helstrom best measurement strategy with the novel Majrana representation. For a  $d$  dimensional state, the Majrana representation defines the state (up to a global phase) by  $d-1$  points on the surface of a Riemann sphere. Geometric interpretation of physical systems is often very helpful in gaining further intuition. For example, the Bloch sphere can be used to see intuitively the way optimal fidelity is achieved in universal quantum cloning [9]. The Majrana representation shows well the changes in the measures affected by changing  $S$  for the spin coherent states in a simple geometry.

Conclusions are finally drawn and comments made about the nature and validity of the results found. We compare the two methods of accessing classicality with each other and other proposed methods. We also suggest a number of further investigations that can be carried out along the lines of the present work.

## II. ACTION THROUGH A BEAM SPLITTER

In optics the action of a beam splitter is described as a particular kind of mixer of two beams of light or, more mathematically, two modes of the quantised electromagnetic field. A 50/50 beam splitter takes an input state comprised of a general  $n$  photon Fock state in one mode and a ground (vacuum) Fock state in the other,  $|j;0\rangle$ , to a superposition of binomially populated modes:

$$U_{bs} |j;0\rangle = \sum_{p=0}^n \frac{X^n}{2^{n/2}} \binom{n}{p}^{1/2} |p;n-p\rangle \quad (1)$$

In general these resultant states will be entangled, indeed, for any input made up of a finite superposition of Fock states the entanglement cannot be zero (except, of course, in the case of the trivial ground state). This can easily be proved by tracing one of the output modes and checking that the resulting state (of the other mode) is strictly mixed, i.e., its trace is less than one. Since we will only deal with overall pure states in our paper, this method for quantifying entanglement will be adequate in general and we will use it later on in this section. We choose a 50/50 beam splitter because it is, in some sense, most efficient at generating entanglement providing we have the above specific scenario of one input arm in the vacuum state (e.g., the input state  $|j;0\rangle$  would be transformed to a maximally entangled Bell state).

A Glauber state is defined as  $|j\rangle = \exp\left(\frac{1}{2} j \hat{J}^2\right) \sum_{n=0}^{\infty} \frac{j^n}{(n!)^{1/2}} |n\rangle$  [10]. When this enters one mode and a ground state the other, the output state is  $|j_{out}\rangle = U_{bs} |j;0\rangle = \exp\left(\frac{1}{2} j \hat{J}^2\right) \sum_{n=0}^{\infty} \frac{j^n}{2^{n/2} (n!)^{1/2}} |n\rangle$  which reduces to the product state  $|j_{out}\rangle = \exp\left(\frac{1}{2} j \hat{J}^2\right) \sum_{p=0}^{\infty} \frac{j^p}{2^{p/2} (p!)^{1/2}} |p\rangle \sum_{n=p}^{\infty} \frac{j^{n-p}}{2^{(n-p)/2} ((n-p)!)^{1/2}} |n-p\rangle = |j\rangle \otimes |j\rangle$ . It

has been proven that the Glauber states are the only states that when passed through one arm of a beam splitter return product states, with no entanglement [3]. Therefore they are the only classical states within this framework.

Although the beam splitter needs to be defined in a more general way (by giving the transformation of the general basis state  $|j; m\rangle$ , or, equally well, by defining the action of annihilation and creation operators on the different modes as in, for example, [11]), it will for us be sufficient to use equation (1) as a specialised definition on the state  $|j; 0\rangle$ . We now ask what action such a beam splitter makes on a spin coherent state and to what extent the output state depends on the magnitude of the spin.

A spin coherent state  $|z\rangle$  is defined here to be the minimum uncertainty, complex rotation of the ground state, parameterised by a complex amplitude  $z$  [6], [7], [4]. In terms of the spin step up operator  $\hat{S}_+$  acting on the ground state, we have that

$$|z\rangle = \frac{1}{(1 + |z|^2)^S} \exp(z\hat{S}_+) |0\rangle \quad (2)$$

Expanding the exponential we get

$$|z\rangle = \frac{1}{(1 + |z|^2)^S} \sum_{n=0}^{2S} \frac{(2S)!}{n!} z^n |n\rangle \quad (3)$$

The summation only goes up to  $2S$  since it is unreasonable to have  $\hat{S}_+$  acting on  $n$  greater than  $n = 2S$ , i.e., we set, for  $m > 2S$ ,  $\hat{S}_+ |m\rangle = 0$ . The uncertainty relation for the spin operators, defined with algebra  $[\hat{S}_i; \hat{S}_j] = i\hat{S}_k$ , is given by

$$\langle \hat{S}_i^2 \rangle \langle \hat{S}_j^2 \rangle \geq \frac{1}{4} \langle \hat{S}_k \rangle^2 \quad (4)$$

This equality holds for the state  $|z\rangle$ , hence the spin coherent states are minimum uncertainty states.

In [6] and [7] it is shown by means of the second quantisation, in terms of the operators generating the state, that the limit takes the spin coherent states to the Glauber states. We now look at this limit purely in terms of the first quantisation, which has the advantage that it allows us to easily generate an infinite set of states that have the same property that they asymptotically approach the Glauber states. With the appropriate amplitude relationship, as  $S$  goes to infinity the spin coherent states represent a subclass of Glauber states, namely, those that are orthogonal. Setting  $z = \sqrt{2S}z$  provides a suitable substitution. To prove the equivalence it is enough to show that the overlap between the Glauber state  $|j\rangle$  and the spin coherent state  $|z^0\rangle$  with this substitution goes to 1 in the infinite  $S$  limit. That is, we wish to prove

$$\begin{aligned} \lim_{S \rightarrow \infty} \langle j | z^0 \rangle &= \lim_{S \rightarrow \infty} \left( \exp \left[ \frac{1}{2} |z|^2 \right] \frac{1}{(1 + \frac{|z|^2}{2S})^S} \sum_{n=0}^{2S} \frac{(2S)!}{(2S-n)!(2S)^n} \frac{|z|^{2n}}{n!} \right) \\ &= 1 \end{aligned} \quad (5)$$

We can see that the normalisation term outside the sum clearly goes to the exponential in the limit. We also see that each term in the sum goes to  $\frac{|z|^{2n}}{n!}$  in the limit. The limit of the sum then gives an inverse exponential. Since both terms converge in the same limit, the product of these terms converges to the product of the convergences and so gives us a product of two exponentials in the limit which cancel to give one. In fact, this is true of any state  $|j\rangle = \sum_{n=0}^{d-1} f(n;d) \frac{A^n}{(n!)^{1-2\alpha}} |n\rangle$  such that  $f(n;d) > 0$ ;  $0 < \alpha < 1$  and  $f(n;d)$  converges to 1 in  $n$  for all  $p$ . There are infinitely many such functions and therefore these states define an infinite set of states that asymptotically approach the Glauber state. A detailed proof can be found in the Appendix (the orthogonality of these states is discussed later). This result shows that in the infinite  $S$  limit, the spin coherent states do not entangle when put through one arm of a beam splitter (since they are in fact Glauber states).

We now wish to see exactly how the entanglement reaches this zero limit. More precisely, we would like to determine if entanglement falls off quickly with increasing spin, such that any reasonably large spin system effectively returns a product state or if, for instance, the drop off is monotonic. The action of a beam splitter on an input state, comprised of a spin coherent state in one mode/arm and the vacuum state in the other, gives

$$U_{bs} |z; 0\rangle = \frac{1}{(1 + |z|^2)^S} \sum_{n=0}^{2S} \frac{(2S)!}{n!} z^n \sum_{p=0}^{2S-n} \frac{(2S-n)!}{p!} z^p |n; p\rangle \quad (6)$$

We use the linear entropy (see, for example, [12]) as our measure for entanglement, defined for a bipartite state  $\rho_{AB}$  as

$$E = 1 - \text{Tr} \rho_A^2; \quad (7)$$

where  $\rho_A = \text{Tr}_B(\rho_{AB})$  is the reduced density matrix of system A. The choice of linear entropy, rather than the normally used Von Neumann entropy [13], is purely for computational ease and is perfectly valid (as is almost any other function of Schmidt coefficients [14]). It too gives a measure of how mixed the local state  $\rho_A$  is, which is essentially a measure of how much information is shared across the state, or how entangled the state is (more precisely the linear entropy of entanglement is a lower bound to the Von Neumann entropy of entanglement). The linear entanglement of the two output "beams" is given by:

$$E = 1 - \frac{1}{(1 + \langle j^2 \rangle)^{4S}} \sum_{p,p^0=0}^{\infty} \frac{2^m \langle j^2 \rangle^m}{m!} \frac{1}{(2S - m - p)!(2S - m - p^0)!} \frac{1}{\rho_A} \frac{2^{-(p+p^0)} \langle j^2 \rangle^{-(p+p^0)}}{p!p^0!}; \quad (8)$$

This is not a closed form solution as it were, so we need to investigate it numerically for qualitative results.

We find that the generated entanglement is very dependent on the amplitude  $z$ , of the input state, and that it falls away very slowly with  $S$ , appearing to only really reach zero in the infinite limit. For a  $\langle j^2 \rangle$  of around one and less, we see a quick initial drop in the entanglement with  $S$ , followed by a very slow tail off, such that it doesn't look like it reduces to zero. For example, in figure 1, where we plot entanglement against  $S$  for  $\langle j^2 \rangle = 1$ . We can see that the entanglement initially falls sharply, followed by a very gradual descent after around  $S = 15$ , such that it hardly appears to decrease, though on closer inspection it does, and we know, must, since in the infinite limit it reaches the zero of the Glauber state. For larger  $\langle j^2 \rangle$  we see an initial peak in the generated entanglement as we increase  $S$ , though again followed by a slowly falling tail. Figure 2 shows an example of this for  $\langle j^2 \rangle = 10$ . In figure 3 we plot the generated entanglement against the spin  $S$  and  $\langle j^2 \rangle$  of the input spin coherent state. We see that the tail off with  $S$  gets higher with increasing  $\langle j^2 \rangle$ , and that the initial peak becomes less pronounced. It looks like the very slow decline with  $S$  will continue beyond the range plotted, so that the zero entanglement generation of the Glauber state is only really seen in the infinite limit. For any fixed  $S$ , as we increase  $\langle j^2 \rangle$  we see a larger generation of entanglement.

The initial peak in generated entanglement, for  $\langle j^2 \rangle$  larger than around one, is best explained by looking at the output, superposition state (6). Roughly speaking, as we increase  $S$ , the addition of entangled states to the superposition causes a growth in entanglement. This is then countered as more states are added, having the effect of diluting the superposition, so that the entanglement goes down for greater  $S$ . We do not see this for  $\langle j^2 \rangle$  less than around one, because the coefficients for the higher entangled states in the superposition decrease for higher orders. We note that a similar phenomenon was seen in [8], where A mesen et al studied the entanglement between two spin  $1=2$  particles in a mixed thermal state with an external magnetic field, according to the antiferromagnetic Heisenberg model. For some field strengths, as the temperature of the chain increased, there was an initial increase in entanglement, though in the large limit the entanglement went down to zero, as we would expect for such a mixed system. The increase can be put down to the inclusion of highly entangled states in the mixture, which then becomes countered as the mixture dilutes as it extends to more states. There is a difference in that in our case the increase came from the addition of states to a pure superposition and in theirs, they are added to the mixture.

We now consider what this means in terms of classicality. This classical feature of the Glauber state, i.e., that of zero entanglement generation when passed through one arm of a beam splitter, is elusive to the spin coherent state, except for those with the highest spin. The infinite  $S$  limit offers the set of "most" classical spin coherent states, since they are equivalent to the Glauber states and hence generate no entanglement. On this ground alone though, the spin coherent states are no more classical than in nitely many other possible sets of states. Then, the fact that we get an increase in entanglement as we increase  $S$ , is surprising, in that it indicates a reduction in classicality. Given this, we may ask if we can think of a state that is more classical in this sense, namely, one that generates less entanglement and for which the entanglement decreases more rapidly with the dimension of the Hilbert space. This is a complicated problem since the only finite dimensional state to give non entangled states through a beam splitter is the ground or vacuum state. The spin coherent states can be arbitrarily close to this zero entanglement, but that is simply because they are arbitrarily close to the ground state in some sense. We then ask how valid this measure of classicality is. For example, we could think of other unitary transformations that would create more entanglement with the input states here, indeed, the amount of entanglement generated for a given transformation is dependent on the input state. We can talk of the entangling capacity of a unitary transformation [15], which is a maximum taken over all input states, however, to define a class of minimum entangling states for one unitary transformation does not mean it is the class of

minimum entangling states for a different unitary transformation. The beam splitter transformation is a very specific example, which is important in showing one classical feature of the Glauber states, but there is no reason to choose this one over other transformations as a general measure. As such, we can claim that this is not an ideal measure, indeed as a concept, the resistance to entanglement generation of a state is not well defined.

It is still interesting in its own right, however, to see how this class of states is affected when passed through one arm of a beam splitter, since beam splitters are among the simplest devices implementable by experiment and have many applications, including entanglement generation itself (for example, [16]); so it is valuable to understand them better in any scenario, especially one involving entanglement generation, as is this one. As an entanglement generator for the specific scenario of a coherent state,  $|z\rangle$ , entering one arm and a vacuum state,  $|0\rangle$ , the other, we can point out some more interesting results about the 50/50 beam splitter. We can see that the higher the amplitude of  $|z\rangle$ , the higher the generated entanglement for any  $S$ . Also, for a given amplitude  $z$  there is a  $S$  that gives a maximal entanglement possible, and this increases with  $|z|$ . For  $|z| < 1$  this is the initial entanglement, for larger  $|z|$ , where we see an initial rise, there is always a maximum since in the limit it falls to zero, this can be clearly seen, for example, for  $|z|^2 = 10$  in figure 2.

It is also informative to consider the physical notion of a beam splitter in the sense described above. In the case of the optical state, when we use the term "beam" we usually mean literally beam, or mode of light, that is defined by the path it takes. The action of the beam splitter is then to split the incoming photons of one mode (or path) into two, so the photons leave in a superposition of both paths. This can be written in terms of the creation and annihilation operators, whence the beam splitter annihilates photons from the input path and creates photons in both output paths. With spin coherent states this is not so clear. The analogous operators to the annihilation and creation operators are the step up and down operators. The analogy of creating a photon in a beam would be to add a unit of spin to the system (though the analogy is not exact because of different commutation relations, which change the beam splitter transformation, but broadly speaking it still accomplishes the same). With this in mind one possible interpretation of a spin  $S$  system is as a symmetric superposition of  $2S$  spin  $1/2$  systems. Hence one can think of beam of spin  $1/2$  particles being split into two paths, where the increase of one unit of spin is equivalent to the addition of a spin  $1/2$  particle. In this way, the addition of more particles increases the total spin and so makes the system more "classical", as it is the case for optical states, where the more photons there are (the higher the amplitude) the more classical the system can be said to be in terms of distinguishability and entanglement (the states out of a beam splitter are only the same as the input in the infinite limit of ). This view of a spin  $S$  system has a natural link to the Majumara representation to be discussed later, since it can be seen as an illustration of these particles.

### III. COHERENT STATE DISCRIMINATION

One of the fundamental principles of quantum mechanics is the uncertainty relation between incompatible observables which, in turn, prohibits us from distinguishing two nonorthogonal states perfectly with one measurement. This strongly contrasts with the classical world where, at least in principle, all states can be distinguished perfectly. We can, however, optimise our measurement strategy in quantum mechanics to give us the most reliable answer possible. One such strategy is that given by Helstrom [17] (see also [18] for a very readable account) where a measurement is made to give two outcomes, one corresponding to each of the states, with a minimal probability of error. We briefly state some of those results before applying them to analysing spin coherent states.

Suppose that we are given a system we know to be in one of two states,  $|A\rangle$  or  $|B\rangle$  with probabilities  $p_A$  and  $p_B$ , respectively. When trying to ascertain which of the two nonorthogonal states we have, we construct a two outcome generalised measurement, or positive operator-valued measure (POVM), made up of  $\hat{E}_A$  and  $\hat{E}_B = \hat{I} - \hat{E}_A$  and associate the states with the corresponding results. The probability of being incorrect in our association  $P_e$ , is given by

$$P_e = p_A \text{tr}(\hat{E}_B |A\rangle\langle A|) + p_B \text{tr}(\hat{E}_A |B\rangle\langle B|): \quad (9)$$

For us it is important that in the case of pure states  $|A\rangle$  and  $|B\rangle$  this POVM becomes a projection measurement with the probability of error given by

$$P_e = p_A \text{tr}(\hat{E}_B |A\rangle\langle A|) + p_B \text{tr}(\hat{E}_A |B\rangle\langle B|): \quad (10)$$

Optimisation of this expression comes through our choice in the projection measurements. Heuristically, we wish to choose the projection spaces of  $\hat{E}_A$  and  $\hat{E}_B$  such that  $|A\rangle$  and  $\hat{E}_B$  are as close to orthogonal as possible, similarly

for  $\beta$ . This must be balanced against the a priori probabilities to give the minimum probability of error. Helstrom showed that the minimum probability of error in discriminating two pure states is given by

$$P_e = \frac{1}{2} \left( 1 - \sqrt{1 - 4p_A p_B |\langle \psi_A | \psi_B \rangle|^2} \right) \quad (11)$$

We now wish to look at this as our measure of distinguishability (or indistinguishability) for spin coherent states. We begin again by looking at the infinite limit. As mentioned earlier, as  $S \rightarrow \infty$ , all spin coherent states become orthogonal, that is the overlap tends to zero. This can be easily seen. Two spin coherent states,  $|j, \alpha\rangle$  and  $|j, \beta\rangle$  have overlap  $\langle j, \alpha | j, \beta \rangle = \frac{j(1+\cos\theta)^{2S}}{j(1+\cos\theta)^S (1+\cos\phi)^S}$ . Since  $j(1+\cos\theta)^2 = j(1+\cos\phi)^2$  the limit in  $S$  gives  $\lim_{S \rightarrow \infty} \langle j, \alpha | j, \beta \rangle = 0$  except when the equality is reached, i.e.,  $\theta = \phi$ , which, for all  $S$ , gives  $\langle j, \alpha | j, \alpha \rangle = 1$ . Thus in the limit of large  $S$  all spin coherent states are orthonormal to each other and hence are entirely distinguishable from one another (as can be seen in equation (11) as  $P_e$  vanishes to zero).

We can then look at how this distinguishability changes with  $S$ . When attempting to distinguish two spin coherent states  $|j, \alpha\rangle$  and  $|j, \beta\rangle$  we get

$$P_e = \frac{1}{2} \left( 1 - \sqrt{1 - 4p_A p_B \frac{(1+\cos\theta)^{2S}}{(1+\cos\phi)^S (1+\cos\psi)^S}} \right) \quad (12)$$

In figure 4 we plot the probability of error against  $S$  for  $\theta = 0$ ,  $\theta = 1$  and  $p_A = p_B = 1/2$  (which, since  $p_A + p_B = 1$ , clearly gives the largest probability of error). We see a very quick decrease in  $P_e$  such that it is negligible by around  $S = 4$ . This trend of rapid decrease remains for all  $\theta$  and  $\phi$  where they are significantly different. To look at this it is sufficient to consider states with  $\theta = 0$  and  $\phi = 2\pi R$  since  $P_e$  depends on the modulus of the overlap. In figure 5 we plot  $P_e$  against  $S$  and  $\theta$  (real), again for  $p_A = p_B = 1/2$  since this is the maximum error and will show the trends best. We see that the smallest  $S$  gives the highest probability of error and the decrease with  $S$  is monotonic for all  $\theta$  (real) (as can be verified easily by looking at equation (12)). We also see that, for all  $S$ , as  $\theta$  gets larger the probability of error decreases, and for  $S > 1$  goes to near zero very quickly. As  $\theta$  approaches  $\pi$ ,  $P_e$  approaches half, that of a random guess, no matter the  $S$ , which we would obviously expect since two equal states can never be told apart. In the interesting region, as  $\theta$  increases away from  $\pi$ , the rapid decrease of  $P_e$  with  $S$  appears very quickly, so that, for all but near zero difference in  $\theta$  and  $\phi$ , the distinguishability emerges very quickly. Plotting the same graph with different  $p_A, p_B$  will give smaller values of  $P_e$  and not change the overall trends.

If we consider classicality purely in terms of this distinguishability, we can say that the spin coherent states have a smooth and quick transition to the classicality of distinguishability of the Glauber states, from the  $S = 1/2$  least classical state, to the infinite limit, which is completely distinguishable thus most classical. Unlike resistance to entanglement, which is not clear as a measurable feature of classicality, distinguishability for a set of states is simply defined here. It is interesting to compare this to the natural curvature of the space of the set of spin coherent states arising from the Fubini-Study metric [19]. The Riemannian curvature  $K$ , given by  $K = \frac{1}{2S}$  is dependant on the size of the spin system. We see that the "least" classical,  $S = 1/2$ , state the curvature is maximal at  $K = 1$ . This reduces smoothly and monotonically with  $S$  until in the infinite limit, for the "most" classical state, the curvature is zero. Hence the curvature of the underlying space seems to be related in some way to the classicality.

One very illuminating way to see the difference in the measurement process as we change  $S$  or  $p_A/p_B$  is to represent the states and the POVMs on the Riemann sphere using the Majorana representation. In this system, a state with spin  $S$  is represented by  $2S$  points on a Riemann sphere. The position of these points is given by the zeros of a complex function, constructed from the overlap of the state with a non-normalised spin coherent state. The overlap between a non-normalised spin coherent state  $|\psi\rangle$  and  $|j, \alpha\rangle$  is given by

$$\langle \psi | j, \alpha \rangle = \sum_n \binom{2S}{n} z^n \quad (13)$$

The general state  $|j, \alpha\rangle = \sum_{n=0}^{2S} a_n |j, \alpha\rangle$  is described (up to a global phase) by the overlap function in  $z$  (also known as the "amplitude function" [7] or the "coherent-state decomposition" [20])

$$\langle \psi | j, \alpha \rangle = \sum_n \binom{2S}{n} a_n z^n \quad (14)$$

$$= \sum_{i=1}^{2S} \langle z | z_i \rangle \quad (15)$$

where  $N$  is simply a normalisation constant.

The zeros of this function describe the state  $|j\rangle$  entirely, again up to a global phase. To plot these points onto the sphere, we view them as stereographic projections from the north pole onto the complex plane going through the equator. Thus a zero on the plane marks the south pole and as the modulus of the root tends to infinity we get a point at the north pole – this happens when  $|z|$  is of order less than the dimension  $d, m$  minus one. The multiplicity of points at the north pole is equal to the difference between the order of  $|z|$  and  $d - 1$ , thus the state  $|j\rangle$  is represented by  $2S$  points at the north pole. The projection of  $z = \frac{e^{i(\theta)}}{\tan(\theta/2)}$  onto the sphere represents the rotation of a point at the north pole through angle  $\theta$  around the axis  $\hat{n} = (\sin(\theta); \cos(\theta); 0)$ , i.e., a point with azimuthal and polar angle  $\theta$  and  $\theta/2$ , respectively. This can also be thought of as representing the rotation  $\hat{R}^{\theta}$ ; on state  $|j\rangle$ .

In the  $S = 1/2$  case we find the well known Bloch sphere. Then, the state  $|j\rangle = \cos(\theta/2)|j\rangle + e^{i\phi} \sin(\theta/2)|j\rangle$  has an overlap function  $\langle z | j \rangle = \cos(\theta/2) + e^{i\phi} \sin(\theta/2)$  with one zero at  $z = \frac{e^{i(\theta+\phi)}}{\tan(\theta/2)}$  where  $\theta$  and  $\phi$  are the polar and azimuthal angles, respectively. We also note that the Majumbara picture could equally represent a multiparticle state of  $2S$  spin  $1/2$  particles in a symmetric superposition. Each point represents one spin  $1/2$  particle [21]. Going back to the notion of a beam of spin  $S = 1/2$  states mentioned in the previous section, each point would then represent a particle in our beam.

We can make a number of observations from this definition. Firstly, spin coherent states are represented by  $2S$  points all at the same one position on the unit 2-sphere. This is clear since for a spin coherent state  $|j\rangle$ , the overlap function is  $\langle z | j \rangle = \frac{(1+z)^{2S}}{(1+jz)^S}$ , which has  $2S$  zeros at  $z = -1$ . Thus, the Majumbara plot of a spin coherent state, can be seen as a representation of the rotation  $\hat{R}^{\theta}$ ; that defines the state  $|j\rangle$ . Secondly, any rotation of a state  $|j\rangle$ , rotates the sphere, since when forming the overlap function (equation (14)), we can equally consider the rotation on  $|z\rangle$  as a reverse rotation on each of the  $|j\rangle$ 's, corresponding to the zeros, which is also a rotation of the points around the sphere. Note though, such a rotation can still add a phase that will not be seen on the Majumbara sphere. This provides the basis for the next two points.

The modulus of the overlap between any two spin coherent states is given entirely by the angle between their points on the sphere. This is true since any two pairs of spin coherent states, with the same angle between them on the Majumbara sphere, are only a unitary rotation apart (up to a phase), since this preserves the overlap up to a phase, any such pairs have equal overlap modulus. Any state with one or more points antipodal to a coherent state is orthogonal to that state. To see this it is sufficient to show it for the case  $|j\rangle = |j\rangle$ , since we can simply rotate the sphere and maintain any overlap up to a phase. The set of states orthogonal to  $|j\rangle$  are given by  $|j^\perp\rangle = \sum_{n=1}^{2S} a_n |j\rangle$ . The coherent state decomposition thus has  $z = 0$  as one of its zeros at least, indeed this can only occur if the state has no components in  $|j\rangle$ . This gives a Majumbara point at the south pole, i.e. antipodal.

With this, we can begin to look at how the Helstrom discrimination strategy for two spin coherent states can be seen in this representation. The states themselves are shown as two points on the sphere. To represent the projections we show the two resultant states after the measurement takes place,  $|j_A\rangle, |j_B\rangle$ , corresponding to  $\hat{E}_A$  and  $\hat{E}_B$ , respectively. We can do this because the two states to be distinguished will both collapse onto the same one of two resultant states. This is because any projection we make will be on the two dimensional subspace of the two states, since to project outside this space would not be optimal. Hence, they project onto the same pair of states in this subspace.

The first thing we notice is that for any  $S$ , these states give Majumbara points that lie on a circle on the surface of the sphere. This is, in fact, the case for any state that is a superposition of two spin coherent states. For any complex coefficients  $a$  and  $b$ , the state  $|j\rangle = a|j\rangle + b|j\rangle$  gives overlap function zeros that lie on a circle of radius  $r = \frac{a}{b} \frac{1-2S}{(1+jz)^{1-2S}}$ , centred at  $z = -1$  on the complex plane. The stereographic projection preserves circles and angles [22], hence the Majumbara points lie on a circle also (since this is true for the above superposition, it is true for any superposition of two coherent states because we can always rotate the pair so that one state is  $|j\rangle$  and maintain the geometry). Furthermore, the radius and position of these circles relate back to the overlap of the states and their a priori probabilities, though the relationships are complicated and we will talk only about trends qualitatively.

In figure 6 we see the Majumbara projection of two spin coherent states, given by two black points, and the states post projection, given by the grey points, that sit on two circles, for  $S = 10$ . State  $|A\rangle = |j\rangle$  sits on the north pole and state  $|B\rangle = |j\rangle$  sits at  $(1; 0; 0)$ . The a priori probabilities are set at  $p_A = p_B = 0.5$ .

We can now look at how when changing the a priori probabilities,  $p_A/p_B$ , and  $S$ , the Helstrom measurements we make, found from the minimisation of equation (11), also change. For any fixed spin, as the a priori probability of  $|A\rangle$  increases, the circle of the corresponding projection  $\hat{E}_A$  closes in around the state, until it becomes that state. That is,  $|j_A\rangle = |A\rangle$ , as we would expect for minimisation of equation (10). The other circle, for projection  $\hat{E}_B$ , widens until it becomes the state orthogonal to  $|A\rangle$  in the  $|A\rangle, |B\rangle$  subspace ( $|A^\perp\rangle$ ), this gives the circle whose width allows one point to sit antipodal to the Majumbara point of  $|A\rangle$ . The opposite to this occurs should  $p_B$  increase.

Keeping  $p_A/p_B$  fixed and increasing  $S$  both circles become larger, as  $|j_A\rangle = |B\rangle$  and  $|j_B\rangle = |A\rangle$ . This shows the reason for the decrease in probability of error with  $S$  seen in figures 4 and 5. As  $S$  increases, the states  $|A\rangle$

and  $\beta_i$  become more orthogonal, this allows the projection POVMs to change to become more orthogonal to the anticorresponding states, in accordance with the minimisation of equation (10), seen by the growth of the circles, where  $P_e$  then reduces with  $S$ . Therefore, the smooth growth of the projection circles illustrates that within this distinguishability criterion for classicality, spin coherent states approach the "classical", Glauber, states with the increase of spin. This is in contrast with the previous criterion based on entanglement generation where we see a brief increase of entanglement with spin.

#### IV. CONCLUSION

In this paper, we have extended the analysis of spin coherent states to examine their transition from spin  $S = 1=2$ , to the limit  $S \rightarrow \infty$ . We gave an alternative proof that, as the spin goes to infinity, the spin coherent states become an orthogonal subset of the optical coherent, Glauber, states. From this proof we can easily see that this is not unique to spin coherent states, indeed there are infinitely many sets of states for which this is true. The spin coherent state does represent an element of these that achieves minimum uncertainty.

We have studied the entanglement generation of spin coherent states for the specific case where they are sent through one arm of a 50/50 beam splitter and a vacuum through the other. We found the entanglement to be very slow in decreasing as  $S$  of the input state increases, and very dependent on amplitude  $z$  of the state. We also found that the entanglement went up initially as we increase  $S$  for  $|z| > 1$ . The high dependence on  $|z|$ , very slow decline to zero and increase of entanglement (thus dip in this sense of classicality) are indicators that this measure may be inadequate as a universal signature of classicality, as we found. The value in these results is in the understanding of a beam splitter as an entanglement generator, with respect to which, it is also found that the generated entanglement increases with amplitude  $z$ , and that for any spin  $S$  we can find an amplitude with  $|z|$  that gives the maximum entanglement at output. In a sense we have sacrificed the generality of this result as a classicality measure for its simplicity and applicability. One possible extension to the work done here on beam splitters, would be to analyse the entanglement generation of spin coherent states under the wider set of compact unitary transformations.

We then looked at the distinguishability of two spin coherent states. The probability in error for the Helstrom measure was used as a measure of how distinguishable the states are. The distinguishability increases for any two states of set amplitude as we increase  $S$ . The classical feature of distinguishability seen for the orthogonal set of Glauber states is seen to be reached quickly and monotonically as we increase from  $S = 1=2$  to  $S \rightarrow \infty$  for the spin coherent states, allowing us to call  $S = 1=2$  least classical, with least distinguishability for any two spin coherent states, and the infinite limit  $S \rightarrow \infty$  most classical, where all states are fully distinguishable hence in this respect classical.

Noting that the this classicality of distinguishability offers a smooth transition from the least  $S = 1=2$  to the most classical  $S \rightarrow \infty$  spin coherent states we can think of other possible measures. One mentioned earlier in the section III, is the curvature of the state space according to the Fubini-Study metric, which for the spin coherent state is given by  $K = \frac{1}{2S}$  [19]. Thus, this also gives a smooth transition with  $S$ , decreasing from the maximal  $K = 1$  for the least classical spin half state, to atness,  $K = 0$ , for the limit (most classical). Unlike the classicality of distinguishability, the curvature does not depend on the amplitude  $z$ , because the (Riemann) sphere is equally curved at all points. Another measure of classicality might be the distance from the Glauber states (using any "reasonable" distance measure), which, for example, monotonically decreases to zero in the infinite limit and is smaller for higher  $z$ . We reiterate that none of these measures give a common result; they all follow different declines and cannot be said to be equivalent exactly in the transition regime. Indeed this by no means offers a complete description of what we mean by classicality, here we simply trace some classical properties of the Glauber states for the spin coherent states through  $S$ .

Finally we used the Majorana representation to illustrate the Helstrom measurement strategy. The geometry of the states and the Helstrom POVMs is simple, and allows us to illustrate easily the changes affecting the probability of error for the measurement. A spin coherent state is simply one point on the sphere and the POVMs are represented by circles of points. The decrease in probability of error with an increase in  $S$  is seen by the increase in the diameter of the circles on the sphere representing the measurements. It also be interesting for future work to create common criteria for 'classicality measures' or indicators of (pure) states. It seems that one common feature that should be in posed is the increase in classicality with the size of a system, or the number of subsystems involved, so that it appears classical in a large macroscopic limit. An important problem, brought to light in the discussion of the beam splitter, is the assignment of classicality in terms of entanglement. A classical system should be inefficient at generating entanglement within itself, but on the other hand, should be able to strongly entangle to its environment (this is required, for example, in decoherence models). It is not at all clear that there exists a single measure that would capture all these desirable properties and this remains a challenging open problem.

Acknowledgements. We would like to thank William Irvine, Manfred Lein and Stefan Scheel for very useful discussions on the subject of this paper and Jens Eisert for critical reading of the proofs involved. This work was sponsored by Engineering and Physical Sciences Research Council, the European Community, the Elsa spa and the Hewlett-Packard company.

- 
- [1] M. Gell-Mann and J. Hartle. *Phys. Rev. D*, 47(3345), 1993.  
 [2] R. J. Glauber. *Phys. Rev.*, 131(2766), 1963.  
 [3] Y. Aharonov, D. Falko, E. Lemer, and H. Pendelton. *Ann. Phys.*, 39(498-512), 1966.  
 [4] J. R. Klauder and B. Skagerstam. *Coherent States*. World Scientific, Singapore, 1985.  
 [5] J. R. Klauder. 2001. Contribution to the 7th ICUSR Conference, June 2001, quant-ph/9601020.  
 [6] J. M. Radcliffe. *J. Phys. A*, 4(313-323), 1971.  
 [7] F. T. Arecchi, E. Courtens, R. Gilmore, and H. Thomas. *Phys. Rev. A*, 6(2211), 1972.  
 [8] M. C. Arnesen, S. Bose, and V. Vedral. *Phys. Rev. Lett.*, 87(017901), 2001.  
 [9] N. Gisin. *Phys. Lett. A*, 242(1), 1998.  
 [10] R. Loudon. *The Quantum Theory of Light*. Oxford University Press, Oxford, 3 edition, 2000.  
 [11] R. A. Campos, B. E. A. Saleh, and M. C. Teich. *Phys. Rev. A*, 40(1371), 1989.  
 [12] S. Bose and V. Vedral. *Phys. Rev. A*, 61(040101), 2000.  
 [13] J. von Neumann. *Mathematical Foundations of Quantum Mechanics*. (Eng. translation by R. T. Beyer), Princeton University Press, Princeton, 1955.  
 [14] G. Vidal. *J. Mod. Opt.*, 47(355), 2000.  
 [15] M. S. Leifer, L. Henderson, and N. Linden. 2002. quant-ph/9601020.  
 [16] S. M. Tan, D. F. Walls, and M. J. Collett. *Phys. Rev. Lett.*, 66(252), 1991.  
 [17] C. W. Helstrom. *Quantum Detection and Estimation Theory*. Academic Press, New York, 1976.  
 [18] C. A. Fuchs. Phd thesis. University of New Mexico, quant-ph/9601020.  
 [19] J. P. Provost and G. Vallee. *Commun. Math. Phys.*, 76(289-301), 1980.  
 [20] P. Leboeuf. *J. Phys. A: Math. Gen.*, 24(4575), 1991.  
 [21] R. Penrose and W. Rindler. *Spinors and Space Time. Vol.1: Two Spinor Calculus and Relative Fields*. Cambridge University Press, Cambridge, check edition, 1984.  
 [22] H. Eves. *A Survey of Geometry*. Allyn and Bacon, Inc. Boston, 1963.

#### APPENDIX A

Glauber states are defined as [10],

$$\begin{aligned} |j\rangle &= \exp\left(\frac{a^\dagger}{2} j\right) |0\rangle; \\ &= \exp\left(\frac{1}{2} j\right) \sum_{n=0}^{\infty} \frac{X^n}{(n!)^{1/2}} |n\rangle; \end{aligned} \quad (\text{A } 1)$$

We wish to show that by appropriate substitution, the spin coherent state (3) is equal to a subclass of Glauber states as  $S$  tends to infinity. We know that for any two, different spin coherent states, the overlap tends to zero as  $S$  tends to infinity, thus the "amplitude" for the optical case must tend to infinity as  $S$  does. We set  $\alpha = \sqrt{2S}z$ . Substituting this into equation (3) we get

$$|j\rangle = \frac{1}{\left(1 + \frac{j}{2S}\right)^S} \sum_{n=0}^{\infty} \frac{X^n}{n!} \frac{(2S)^{1/2}}{2S} |n\rangle; \quad (\text{A } 2)$$

To prove the equivalence of the two states in the infinite limit, it is sufficient to show that the overlap of a Glauber state  $|j\rangle$  and such a spin coherent state goes to one (i.e., they are the same state). Thus, we wish to prove:

$$\begin{aligned} \lim_{S \rightarrow \infty} \langle j | |j\rangle &= \lim_{S \rightarrow \infty} \left( \exp\left(\frac{1}{2} j\right) \sum_{n=0}^{\infty} \frac{1}{\left(1 + \frac{j}{2S}\right)^S} \frac{X^n}{n!} \frac{(2S)!}{(2S-n)!(2S)^n} \frac{j^{2n}}{n!} \right); \\ &= 1; \end{aligned} \quad (\text{A } 3)$$

Let us first look at the summation.  
 Lemma For all  $A \geq 0$

$$\lim_{n \rightarrow \infty} \sum_{p=0}^n \frac{n!}{(n-p)! h^p} \frac{A^p}{p!} = \sum_{p=0}^{\infty} \frac{A^p}{p!} \quad (\text{A 4})$$

Proof We will use the method of showing that the upper and lower bounds to  $\langle z^0 \rangle_i$  coincide as  $S$  tends to infinity. Since each term in the sum is positive, one upper bound of the left hand side of equation (A 4) can be found by taking the sum to infinity. Thus

$$\begin{aligned} \lim_{n \rightarrow \infty} \sum_{p=0}^n \frac{n!}{(n-p)! h^p} \frac{A^p}{p!} &= \lim_{n \rightarrow \infty} \sum_{p=0}^{\infty} \frac{n!}{(n-p)! h^p} \frac{A^p}{p!}; \\ &= \sum_{p=0}^{\infty} \frac{A^p}{p!}; \end{aligned} \quad (\text{A 5})$$

where the last line is given by taking the limit inside the sum, which we are allowed to do since each term converges. We then find a lower bound by taking the sum to some finite  $m$ , so

$$\lim_{n \rightarrow \infty} \sum_{p=0}^n \frac{n!}{(n-p)! h^p} \frac{A^p}{p!} \geq \lim_{n \rightarrow \infty} \sum_{p=0}^m \frac{n!}{(n-p)! h^p} \frac{A^p}{p!} \quad (\text{A 6})$$

However, taking the infinite limit of  $m$  this inequality still holds, since it is true for any finite  $m$  and so it is true for any arbitrarily small distance from the limit so the limit can at most be equal. This gives the same upper as lower bound, hence:

$$\begin{aligned} \lim_{n \rightarrow \infty} \sum_{p=0}^n \frac{n!}{(n-p)! h^p} \frac{A^p}{p!} &= \lim_{n \rightarrow \infty} \sum_{p=0}^{\infty} \frac{n!}{(n-p)! h^p} \frac{A^p}{p!}; \\ &= \sum_{p=0}^{\infty} \frac{A^p}{p!}; \\ &= \exp(A); \end{aligned} \quad (\text{A 7})$$

Since the normalisation and the summation in equation (A 3) converge with  $n$ , the limit of the product is the product of the limits and thus

$$\begin{aligned} \lim_{S \rightarrow \infty} \langle z^0 \rangle_i &= \exp(-j^2) \exp(j^2); \\ &= 1; \end{aligned} \quad (\text{A 8})$$

Interestingly, this is also true of any state  $j$  if  $i = \sum_{n=0}^{\infty} f(n;d) \frac{A^n}{(n!)^{1+2}} |j\rangle_i$  such that  $f(n;d) > 0; \forall n; d \in \mathbb{N}$  and  $f(n;d)$  converges to 1 in  $n$ , for all  $p$ , for example,  $|j\rangle_i = \exp\left(-\frac{1}{2} j^2\right) \sum_{p=0}^{\infty} \frac{z^p}{p!} |j\rangle_i$ . There are infinitely many such functions and therefore there are infinitely many states that will limit to the Glauber state, as stated in section II.

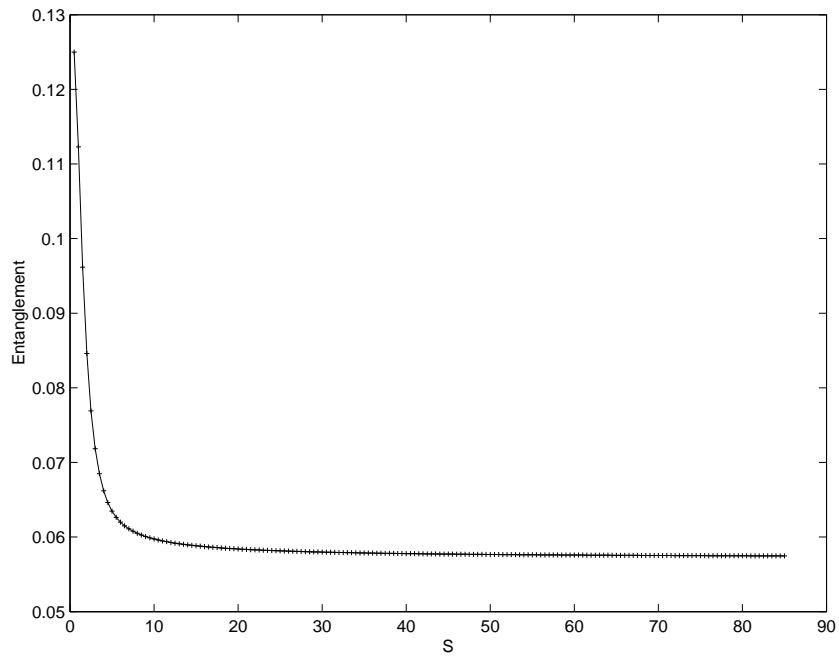


FIG. 1: Linear entropy of entanglement of the state  $|j;0\rangle$  after being passed through a beam splitter, against  $S$  for  $j_f = 1$ . As we can see the entanglement reduces quickly at first but then more slowly. Indeed it does not appear straight away to limit to zero (though we know it does).

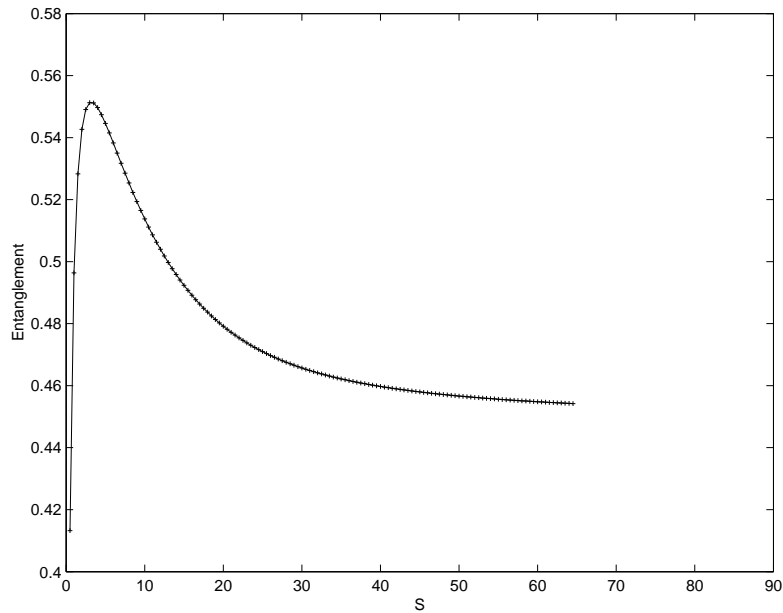


FIG. 2: Linear entropy of entanglement of the state  $|j;0\rangle$  after being passed through a beam splitter, against  $S$  for  $j_f = 10$ . Here the entanglement rises first then tails off after around  $S = 40$ .

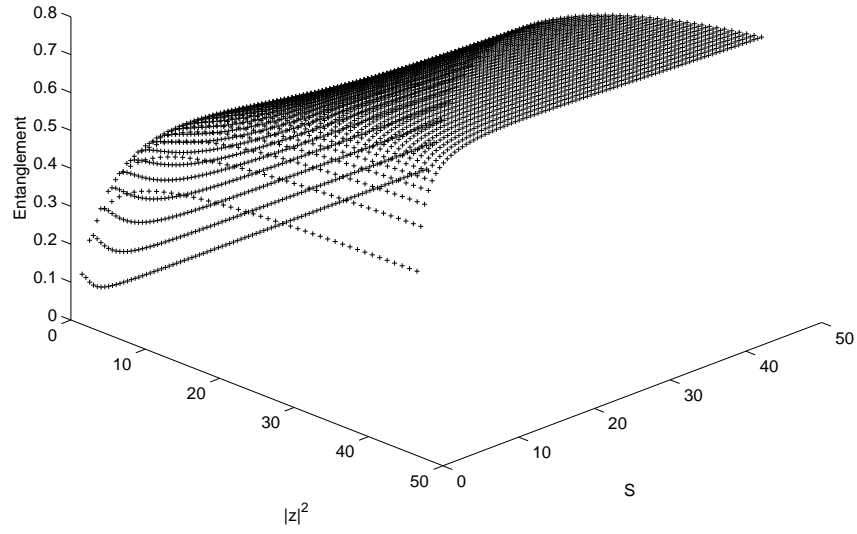


FIG . 3: Linear entropy of entanglement of the state  $|z;0\rangle$  after being passed through a beam splitter, against  $S$  and  $|z|^2$ . We see the pattern of a rapid initial peak followed by very slow decrease thereafter for all  $|z|^2$ , and that an increase in  $|z|^2$  increases the entanglement for any  $S$ .

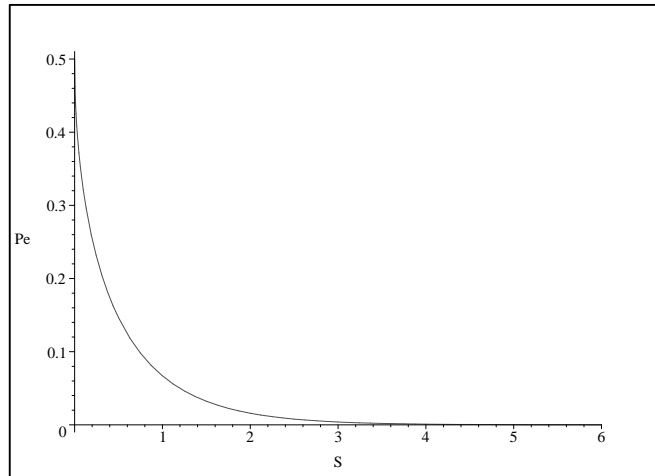


FIG . 4: Probability of error against  $S$  for  $p_A = 0.5$  and  $\theta = 0, \phi = 1$ . The likelihood of error quickly decreases with  $S$ .

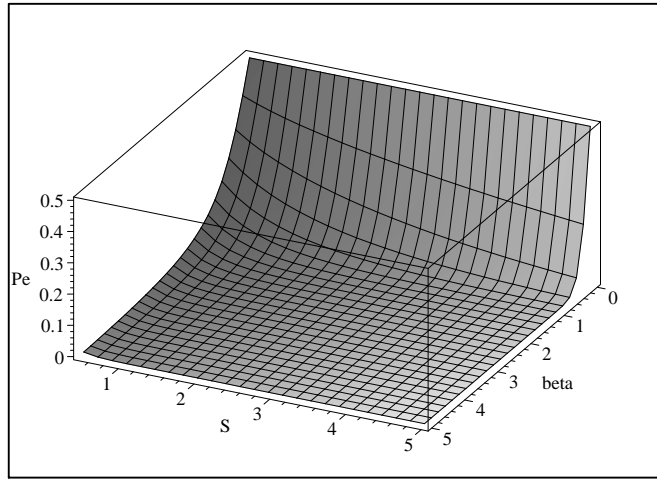


FIG . 5: Probability of error against  $S$  and  $\beta$  (real) for  $p_A = 0.5$ . The likelihood of error quickly decreases with  $S$  for all  $\beta$ .

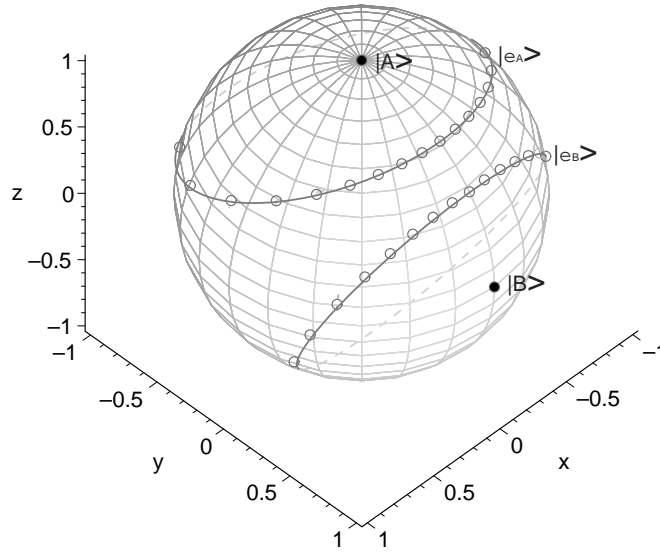


FIG . 6: Bloch sphere projection of two coherent states  $|A\rangle$  and  $|B\rangle$ , and the states post projection  $|e_A\rangle$  and  $|e_B\rangle$ , for  $S = 10$  and  $p_A = p_B = 0.5$ .